

MODIFICATION OF 1D BALLISTIC TRANSPORT USING AN ATOMIC FORCE MICROSCOPE

R. CROOK, C.G. SMITH, M.Y. SIMMONS, D.A. RITCHIE

October 16, 2018

Department of Physics, Cavendish Laboratory, Madingley Road,
Cambridge, CB3 0HE, United Kingdom

Abstract

We have used the scanning charged tip of an Atomic Force Microscope (AFM) to produce images of the conductance variation of a quantised 1D ballistic channel. The channel was formed using electron beam defined 700 nm wide split gate surface electrodes over a high mobility GaAs/AlGaAs heterostructure with a two dimensional electron gas (2DEG) 98 nm beneath the surface. We operate the AFM at 1.5 K and 4.2 K in magnetic fields up to 2 T to observe several phenomena. With a dc voltage on the AFM tip we have produced conduction images of the tip potential perturbation, as the channel is a sensitive probe of the electrostatic potential. We have also performed gate sweeps with the tip at a series of points across the width of the channel. The observed structure in transconductance corresponds to the theoretical electron density for the first three sub-bands. When certain gates were biased near pinch off, stable two level switching was observed in the images. We were able to control the state of the switch with the gate bias and tip position, and so roughly locate the position of the switching source. One of the responsible defect systems was located beneath the 2DEG, and due to screening of the tip potential, the image reveals the 1D channel. By asymmetrically biasing the two gate electrodes we have produced images showing a total channel movement of 102 nm across the width of the channel, but accompanied by 201 nm of movement along the length of the channel which is due to imperfections in the surface electrodes and disorder in the doping layer.

1 Introduction

Recent advances in low temperature Scanning Probe Microscopy (SPM) technology and the availability of high mobility 2DEGs has made possible the imaging of several quantum phenomena. Images of 2DEG electron compressibility in

the quantum Hall state have been produced [1], and a single electron transistor (SET) has been manufactured on a glass tip to detect static charge [2]. The charged tip AFM has been used to locally perturb the 2DEG electrostatic potential, to cause electron backscattering through a 1D channel, and so image the ballistic electron flux [3]. Numerical calculations of the electric field from a conical tip have shown that the half maximum perturbation occurs at a radial distance approximately equal to the 2DEG depth [3], which limits the spacial resolution of this technique.

2 Experiment

In this paper we present images produced by recording the conductance or transconductance through a two terminal 1D ballistic channel, as a charged AFM tip is scanned over the channel region. The 1D channel was created in a 2DEG at a GaAs/AlGaAs heterojunction 98 nm beneath the surface, with a $12 \times 10^{18} \text{ cm}^{-3}$ Si doped layer from 40 nm to 80 nm above the 2DEG. From Shubnikov-deHaas measurements the carrier concentration was calculated as $2.4 \times 10^{11} \text{ cm}^{-2}$ with an electron mean free path of 25 μm . The 1D channel was defined by locally depleting electrons from the 2DEG beneath negatively biased 700nm wide split gate surface electrodes. The surface electrodes extend 30nm above the GaAs surface, and were manufactured using e-beam technology. Our AFM operates from room temperature to 1.5 K, and uses a piezoresistive tip [4] because of the complications of making optical measurements of deflection at low temperatures with light sensitive devices. The AFM operates in the conventional topographic mode to locate the split gate region. During the measurements the AFM force feedback is disconnected and the tip scans a constant height above the surface.

We use two experimental configurations to produce images which are referred to as conductance images and transconductance images. In both configurations a lock-in amplifier measures the ac zero phase component of the channel drain current. For conductance images the ac voltage signal was connected to the channel source with a dc bias applied to the conductive AFM tip. For transconductance images the ac signal was connected to the tip with a dc bias applied to the channel source. The channel conductance is a function of V_{gate} , so for useful transconductance images we operate within a range of G where dG/dV_{gate} remains almost constant.

3 Results and discussion

3.1 Images of the tip perturbing potential

In fig. 1 we present conductance images where the tip scanned a constant 60nm above the surface. In (b) a +2.5 V bias was applied to the tip while in (c) -2.5 V was applied, with a 0.1 mV ac signal applied to the channel source. The channel conductance is a sensitive probe of the electrostatic potential [5],

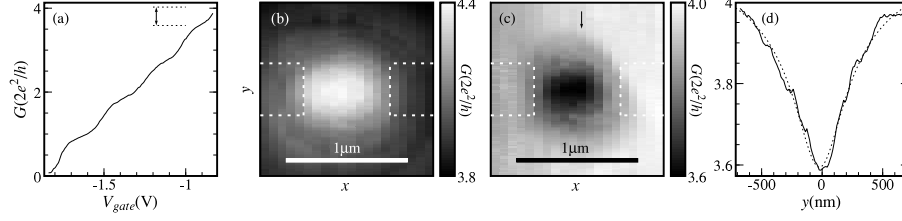


Figure 1: Conductance images of the perturbing potential with a tip bias of +2.5 V in (b) and -2.5 V in (c). A gate sweep is shown in (a) where the tip was off the surface. A y-direction single sweep indicated by the arrow in (c) is reproduced in (d), where the dotted line shows the result of fitting $V_{tip}/\sqrt{\rho^2 + (d + r_{tip})^2}$ to the curve.

so these images reveal the tip perturbing potential at the 2DEG layer. Fig. 1 (a) shows a gate sweep made with the tip away from the surface, where the dotted lines correspond to the conductance range seen in (c). If we model the tip as a spherical charge of radius r_{tip} then at a distance d below the tip we have $U \propto V_{tip}/\sqrt{\rho^2 + (d + r_{tip})^2}$ where ρ is the radial distance in the 2DEG plane. Fitting this equation to the y-direction single sweep shown in (d), which is indicated by the arrow in conductance image (c), provides a good fit with $d + r_{tip} = 230$ nm. Including a correction for the change in relative permittivity, we obtain $r_{tip} = 127$ nm which is in agreement with observations from topological images.

3.2 Measurement of charge density across the channel width

In fig. 2 (a) we present a contour plot which relates to the charge density across the width of a quantised 1D channel. The AFM was positioned at a series of points across the width of the channel (x axis), and at each point the transconductance was recorded (z axis) while the gate bias was swept from -2 V to channel pinch off (y axis). The series of points passed through the channel centre which was located using images like those of fig. 1. The data of fig. 2 (a) has been smoothed in the y direction to remove small steps caused by switching. The wavefunctions, and charge density, for the infinite 1D channel with parabolic confinement are well known and shown in fig. 2 (b), where the spacing between the charge density peaks is roughly equal to half the electron wavelength λ . When we introduce the tip perturbing potential to modify the confining potential, the energy levels change by δE as shown in (c) for a deep 2DEG, and in (d) for a shallow 2DEG, as a function of tip position x_{tip} across the width of the channel. Note that the peaks in the charge density plots also appear in the same positions on the corresponding δE plots, but convolved with the curve of the perturbing potential. The significance of the charge density peaks depends on the width of the perturbing potential, and the model predicts that the $n = 1$

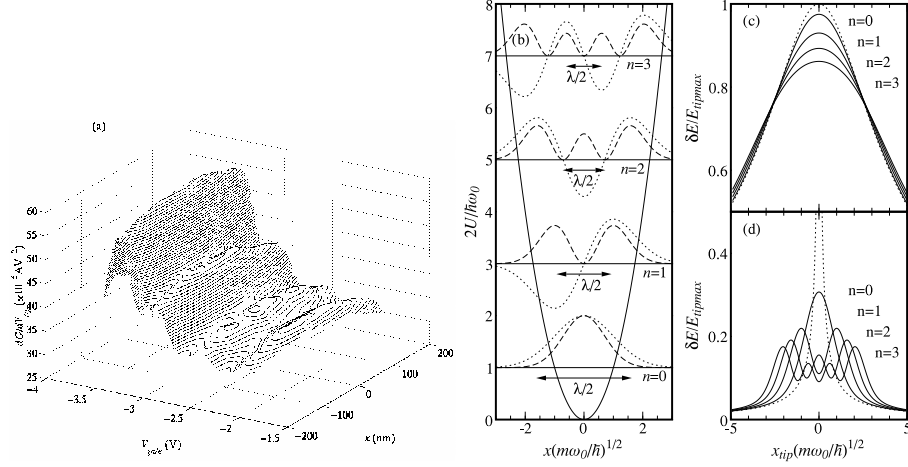


Figure 2: A contour plot of transconductance is given in (a) where the gate bias was swept at a series of points across the width of a ballistic channel. The analytic wavefunctions, electron density, energy levels, and parabolic confining potential are shown in (b), for an infinitely long 1D channel. The model tip perturbation is shown as a dotted line in (c), for a deep 2DEG with $d = 3(m\omega_0/\hbar)^{0.5}$, and in (d), for a shallow 2DEG with $d = 0.1(m\omega_0/\hbar)^{0.5}$, where the solid lines are the resulting perturbed energy levels for $n = 0, 1, 2$, and 3.

peaks will no longer be observed when $d > 1.2(m\omega_0/\hbar)^{0.5}$ or $d > 0.3\lambda$, although increased broadening for higher sub-bands is still predicted.

An ac signal is applied to the tip which oscillates the energy levels. Each energy level determines the gate voltage of the corresponding transition between 1D plateaus. With V_{gate} kept constant, the measured transconductance is proportional to a product of the conductance against V_{gate} gradient and δE . Alternatively, the charge density may modulate the capacitive coupling between the tip and the 1DEG to produce a similar response in transconductance. The distinct peaks in the y-direction of (a) are due the transconductance of 1D quantisation where a peak corresponds to a transition between 1D sub-bands and a trough to a 1D plateau. On top of the distinct peaks we observe weak oscillations in the x-direction where one, two, and three peaks are seen for corresponding transitions of up to one, two, and three sub-bands, which we interpret as a measure of the charge density across the width of a quantised 1D channel. The $n = 1$ peaks are separated by approximately 100 nm, giving an electron wavelength larger than the 2DEG Fermi wavelength due to the reduced electron effective energy and a finite longitudinal momentum in the channel.

3.3 Images of switching states

Switching between stable states in semiconductor devices is frequently observed as a function of time and is known as a Random Telegraph Signal (RTS). When the time constant of the measurement is longer than the switching period a time average of the RTS is measured, which can cause a small ‘plateau feature’ seen in conductance during gate bias sweeps of 1D channels [6, 7]. A RTS observed in channel conduction is believed to be caused by the probabilistic occupation of a nearby defect state by an electron originating in the 2DEG, which then modifies the channel conduction by electrostatics. Fig. 3 (a) and (d) show gate sweeps where the dotted lines indicate the conductance range of the corresponding conductance images (b) and (e). Within the conductance range a small ‘plateau’ can be seen on both of the gate sweeps, characteristic of switching. The position of the AFM tip also affects the defect state occupation which is observed in the conductance images as two levels with a sharp transition. Two levels are visible in (b) as a brighter region in the centre, and in (e) as two darker regions around the ends of the gate electrodes. Fig. 3 (c) and (f) show single y direction sweeps taken from the corresponding conductance images where they are indicated by arrows. The switch step size is constant over each image at $3.8 \mu\text{S}$ for (b), which would require a change of 9.3mV in V_{gate} to produce an equivalent effect. We estimate that a change in gate bias corresponds to 13.3 meV/V change in channel potential [8], which gives an energy change of $120 \mu\text{eV}$ due to the switch. From the conductance image we know the defect is located approximately 100 nm from the channel centre, and probably in the donor layer between 40 nm and 80 nm above the 2DEG plane. If the occupation of the defect state is modelled as a point electron source, then to provide the correct energy change the electron is required to be $1 \mu\text{m}$ from the channel, and although screening has been ignored, the model is poor.

We propose that the source of the switch is a single electron hopping between two nearby defect states. Possible locations for these defects are indicated on the conductance image by \circ and \bullet , where \circ is occupied to produce the background level. The defects are at positions $z_{\circ} = 60 \text{ nm}$ and $z_{\bullet} = 64 \text{ nm}$ above the 2DEG plane, and are separated by 10.5 nm which is of the order of the average dopant spacing at 4.3 nm and near the effective Bohr radius for GaAs.

The two dark switched regions of (e) have the same energy change which suggests that they originate from the same defect system. When the tip is positioned over the channel, and the nearby 2DEG, the switch remains in the background state. This suggests that this defect system is physically below the channel where electrons in the channel and 2DEG provide screening. Again two defect states are required to provide the correct energy change of about $100 \mu\text{eV}$, at possible $z_{\circ} = -110 \text{ nm}$ and $z_{\bullet} = -100 \text{ nm}$, and indicated on the image with \odot as $x_{\circ} = x_{\bullet}$ and $y_{\circ} = y_{\bullet}$. When the tip is positioned near the gate electrode ends where the 2DEG is depleted, the tip potential can penetrate behind the channel, raising the potential of state \circ relative to state \bullet , as state \bullet is closer to the channel and is more effectively screened. Further from the channel, but where the 2DEG is still depleted, the tip has less effect and state \circ is again

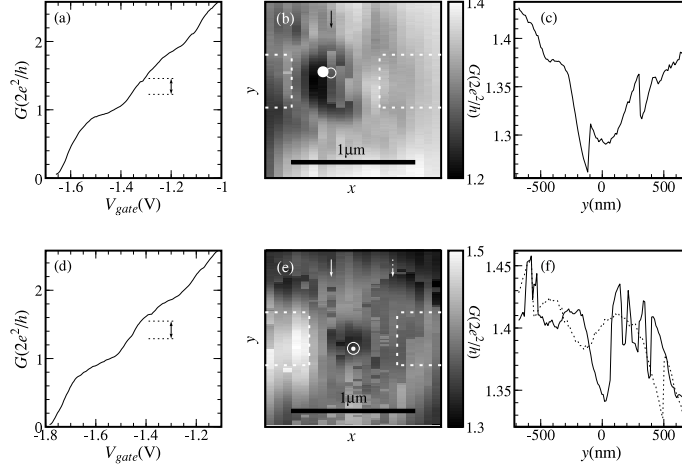


Figure 3: Gate sweeps are given in (a) and (d) where the conductance range of the corresponding conductance images (b) and (e) are indicated by the dotted lines. The arrows on the conductance images indicate the y direction single sweeps shown in (c) and (f).

occupied.

3.4 Images of channel movement due to asymmetric gate bias

For the previous experiments both gate electrodes were biased to the same potential. By asymmetrically biasing the surface electrodes we observe movement of the channel centre in conductance images. Channel lateral position has been studied theoretically [9], and a total movement of $\Delta x = 100$ nm has been deduced by the effect of a defect within the channel [10], though this enabled the channel centre position to be measured in only one direction. For this experiment we used a slightly wider 800 nm split gate orientated in the y direction, but on the same device and with the same AFM tip. Fig. 4 shows three conductance images made with asymmetric gate biases $\Delta V_{gate} = V_{upper} - V_{lower}$ of 3.55 V, 0 V, and -4.27 V respectively, with average gate biases $\bar{V}_{gate} = (V_{upper} + V_{lower})/2$ of -3.14 V, -2.92 V, and -3.06 V set to obtain the same initial conductance. Note that these images were produced consecutively in the order (b), (c), then (a) to avoid the possibility of misinterpreting mechanical drift as channel movement. The channel centre was determined in both the x and y directions by fitting a parabola to the region around the conductance minima. Fig. 4 (d), (e), and (f) show y direction single sweeps reproduced from the respective conductance images where they are indicated by arrows, and were selected to include the channel centre in the x direction. As is

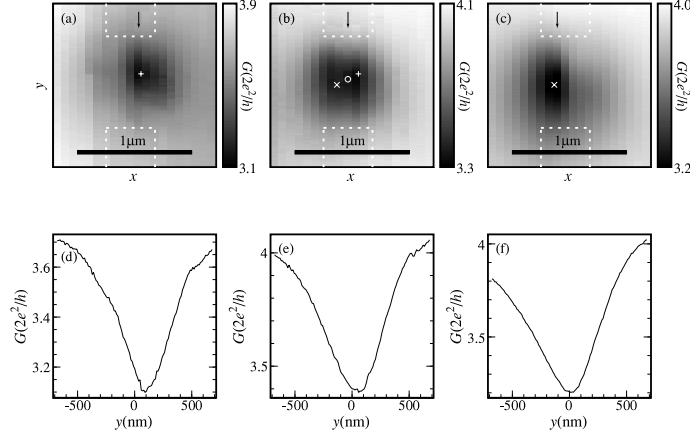


Figure 4: The conductance images (a), (b), and (c) were made with the asymmetrically biased gate electrodes (V_{upper}, V_{lower}) of $(-1.36 \text{ V}, -4.91 \text{ V})$, $(-2.92 \text{ V}, -2.92 \text{ V})$, and $(-5.19 \text{ V}, -0.92 \text{ V})$, with the channel centre $(\Delta x, \Delta y)$ relative to \circ measured at $(98 \text{ nm}, 52 \text{ nm})$, $(0 \text{ nm}, 0 \text{ nm})$, and $(-103 \text{ nm}, -50 \text{ nm})$ respectively. Single sweeps from the conduction images, where they are indicated by arrows, are reproduced in (d), (e), and (f).

evident from the single sweeps the perturbing potential is itself not symmetric, which is why a fit to $V_{tip}/\sqrt{\rho^2 + (d + r_{tip})^2}$ was rejected, and is probably caused by screening of the tip potential by the surface electrodes. The channel centres are indicated on the conductance images by $+$, \circ , and \times at positions relative to \circ of $(98 \text{ nm}, 52 \text{ nm})$, $(0 \text{ nm}, 0 \text{ nm})$, and $(-103 \text{ nm}, -50 \text{ nm})$. The unexpected channel movement in the x direction is caused by imperfections in the surface electrodes, or disorder from the doped layer, which lead to imperfections in the confining potential. The effect is principally seen in the x direction due to the much smaller x component of the confining potential gradient, and therefore increased sensitivity to confining potential imperfections.

4 Conclusion

We have used a conductive AFM tip to modify the conductance of a 1D ballistic channel. By modelling the tip as a spherical charge we obtain a good fit to the observed tip potential perturbation. We have made measurements which reveal structure across the width of the channel, corresponding to the predicted charge density for one, two, and three sub-bands. We have produced images with two levels due to an electron hopping between defect states. When the defect system was beneath the 2DEG plane we obtained images revealing the 1D channel which screened the tip potential. We have observed channel movement when the surface electrodes were biased asymmetrically. Movement along the length

of the channel is believed to be due to electrode imperfections.

Acknowledgments

This work was funded by the EPSRC and the RW Paul Instrument Fund.

References

- [1] S. H. Tessmer, P. I. Glicofridis, R. C. Ashoori, L. S. Leviotov, and M. R. Melloch, *Nature* **392**, 51 (1998).
- [2] M. J. Yoo, T. A. Fulton, H. F. Hess, R. L. Willett, L. N. Dunkleberger, R. J. Cjocjester, L. N. Pfeiffer, and K. W. West, *Science* **276**, 579 (1997).
- [3] M. A. Eriksson, R. G. Beck, M. Topinka, J. A. Katine, R. M. Westervelt, K. L. Campman, and A. C. Gossard, *Appl. Phys. Lett.* **69**, 671 (1996).
- [4] Park Scientific instruments, Sunnyvale, CA 94089, U. S. A.
- [5] M. Field, C. G. Smith, M. Pepper, D. A. Ritchie, J. E. F. Frost, G. A. C. Jones, and D. G. Hasko *Phys. Rev. Lett.* **70**, 1311 (1993).
- [6] D. H. Cobden, N. K. Patel, M. Pepper, D. A. Ritchie, J. E. F. Frost, and G. A. C. Jones, *Phys. Rev. B* **44**, 1938 (1991).
- [7] D. H. Cobden, A. Savchenko, M. Pepper, N. K. Patel, D. A. Ritchie, J. E. F. Frost, and G. A. C. Jones, *Phys. Rev. Lett.* **69**, 502 (1992).
- [8] K. J. Thomas, M. Y. Simmons, J. T. Nicholls, D. R. Mace, M. Pepper, and D. A. Ritchie *Appl. Phys. Lett.* **67**, 109 (1995).
- [9] L. I. Glazman and I. A. Larkin, *Semicond. Sci. Technol.* **6**, 32 (1991).
- [10] J. G. Williamson, C. E. Timmering, C. J. P. M. Harmans, J. J. Harris, and C. T. Foxon, *Phys. Rev. B* **42**, 7675 (1990).